

Article

Stability of Reinforced Retaining Wall under Seismic Loads

Liang Jia ¹, Shikai He ¹, Na Li ² , Wei Wang ²  and Kai Yao ^{3,*} 

¹ College of Civil Engineering, Lanzhou University of Technology, Lanzhou 730050, China; jialiang1949@163.com (L.J.); herryadam@163.com (S.H.)

² School of Civil Engineering, Shaoxing University, Shaoxing 312000, China; lina@usx.edu.cn (N.L.); wellswang@usx.edu.cn (W.W.)

³ Department of Civil & Environmental Engineering, National University of Singapore, Singapore 117576, Singapore

* Correspondence: yaokai@u.nus.edu; Tel.: +65-90592451

Received: 11 April 2019; Accepted: 24 May 2019; Published: 28 May 2019



Abstract: Based on the horizontal slice method (HSM) and assuming a log spiral slip surface, a method to analyze the stability of a reinforced retaining wall under seismic loads was established in this study by calculating the tensile force of the reinforcement. A parametric study was conducted on the normalized tensile force of the reinforcement, and it was observed that the normalized tensile force tends to increase with acceleration of the seismic load and the height of the backfill. Moreover, it also increases with soil unit weight, while it decreases with increased friction angle of the backfill soil, and the influence of soil cohesion on the normalized tensile force is not significant. The HSM method is proved to be suitable for analyzing the tensile force of reinforcement in retaining walls under seismic loads.

Keywords: seismic loads; retaining wall; sliding failure; horizontal slice method

1. Introduction

The reinforced retaining wall is a composite structure widely adopted in seismic regions due to its excellent deformation characteristics under seismic loads, such as earthquakes, owing to the friction between the reinforcement and the soil [1–10]. Okabe [11] proposed the Mononobe–Okabe method, which has been applied in analyzing the stability of reinforced retaining walls under dynamic loads [12]. Zeng and Steedman [13] studied the propagation of the shear wave in the backfill of a retaining wall by the pseudodynamic method and validated the analysis by centrifuge tests. Based on the pseudostatic method, Ling and Leshchinsky [14] and Kwak [15] investigated the vertical seismic response of reinforced soil structures under earthquake conditions. Shahgoli et al. [16] adopted the horizontal slice method (HSM) to analyze the stability of reinforced soil structures subjected to seismic loads. Choudhury and Singh [17] used the pseudostatic method to calculate the active earth pressure behind a retaining wall under seismic load. The slip surface of the reinforced retaining wall was also detected by vibration table tests [18,19], and it was found that the slip surface was like a log spiral. However, the mechanism of collaboration between reinforcement and soil remains unclear. Calculation of the tensile force of the reinforcement is still far from being fully understood and established [20,21]. Based on HSM and log spiral slip surface [16,22,23], the collaborative work of reinforcement and soils is considered in this study to establish a method of analyzing the stability of a reinforced retaining wall under seismic loads. Calculation of the tensile force of the reinforcement is carried out by considering the influence of soil parameters and loading conditions [24,25]. The slice method is proposed to determine the critical failure angle of the backfill wedge under complex conditions, and an iterative

calculation method is presented to determine the tension crack depth of the active earth pressure under seismic loads [26,27]. The axial stress of the anchor is greatly increased by seismic excitation, and the increment is mainly induced within the excitation period of great acceleration amplitude, evaluation of the effect of earthquake frequency content on seismic behavior of cantilever retaining wall including soil–structure interaction [28,29]. By taking the failure surface as a plane, the analytical expression for the critical angle of the failure surface, earthquake-induced displacements of gravity retaining walls and anchor-reinforced slopes are also derived [30,31].

A critical review of literature shows that a very few studies have been reported for the stability analysis of a reinforced retaining wall. The present paper extends the latter work by developing a number of formulations, including a pseudostatic method of analysis. The formulations are described and compared with other published methods used for the seismic analysis of reinforced soil structures. However, no study seems to be available to quantify the effect of seismic acceleration coefficients and soil and reinforcing structure on the stability of reinforced soil walls. In view of this observation, the present study is directed to conduct a seismic stability analysis of the reinforced retaining wall using the HSM and considering the pseudo static forces. The limit equilibrium equation of a reinforced retaining wall under seismic loads is established, and the formula for calculating the tensile force in reinforcement is proposed to address the stability of reinforced retaining wall. In the end, the parametric study has been carried out to investigate the effect of various parameters like reinforcing structure, angle of internal friction and cohesion of soil, horizontal seismic loading.

2. Assumptions and Formulation of the Horizontal Slice Method (HSM)

2.1. Basic Assumptions of HSM

In the HSM approach, the sliding wedge is divided into horizontal slices with rigid-plastic behavior. The seismic force is considered as a pseudostatic force acting at the center of gravity of each slice [23]. The geotechnical interaction between the reinforcing structure and the surrounding soil is ignored. The assumptions are as follows:

- (1) The log spiral slip surface line of the reinforced retaining wall passes through the toe of the wall.
- (2) The sliding body of the retaining wall is divided into several horizontal slices, the number of which is equal to that of reinforcement layers, and each slice contains reinforcement [32].
- (3) The horizontal shear force between reinforcements is ignored.
- (4) The safety factor is assumed to be equal for various slices [23].
- (5) Both horizontal and vertical seismic actions are applied to the center of gravity of the slice.
- (6) The analysis is done by the limited equilibrium method.
- (7) The anchoring strength of the reinforcement and the resistance of the reinforcement against pulling out are not taken into account.

2.2. Formulation of the HSM

HSM was proposed by Lo and Xu [22] and was aimed at overcoming the difficulties in analyzing reinforced soil structures by the vertical slice method (Figure 1). In Figure 1, H is the height of the retaining wall (in m); $S_{y,j}$ denotes the vertical distance between the reinforcement of layer j and layer $j+1$ (in m), and it is usually treated as a certain value in the design; $S_{t,i}$ and $N_{N,i}$ are the shear force and normal force acting on the i th slice, respectively; l_{ai} is the length of reinforcement in the slip zone behind the wall; and l_{ei} refers to the length of reinforcement in the anchorage zone. Figure 2 zooms in on the i th slice taken from Figure 1, which contains one reinforcement. In the figure, $F_{N,i}$ and $F_{N,i+1}$ represent the normal force acting on the top and bottom of the i th slice, respectively; T_i refers to the tensile force of the i th reinforcement [33]; Q_{hi} and Q_{vi} denote horizontal and vertical seismic force, respectively, acting on the top of the slice; α_i is the inclination angle of slip surface of the slice in the horizontal direction; and W_i is the weight of the i th slice. It should be noted that the slip surface is

assumed to be a log spiral shape passing through the toe of the wall [34]. The sliding wedge is assumed to be in a limited equilibrium state, while both horizontal and vertical seismic loads are applied on the center of gravity of the slice. Then the safety for each slice is:

$$F_s = \frac{\tau_f}{\tau_r} \tag{1}$$

where τ_f and τ_r refer to shear strength and shear stress on the sliding surface, respectively.

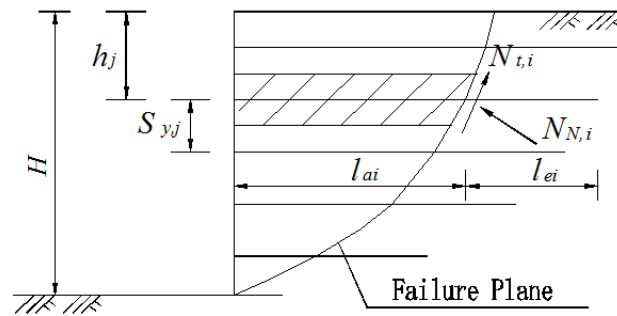


Figure 1. Illustration of failure mechanism of reinforced wall by the horizontal slice method (HSM) (modified after Jia et al. 2018).

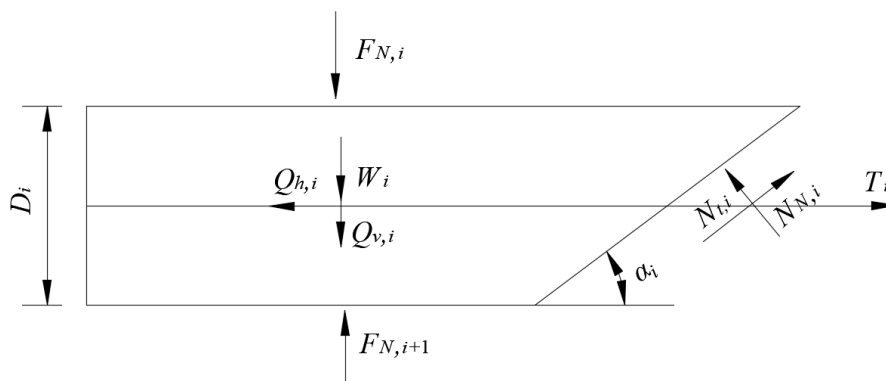


Figure 2. Forces acting on the *i*th slice (modified after Jia et al. 2018).

3. Seismic Loads

Under seismic loads, the shear wave velocity V_s and compression wave velocity V_p are characterized as:

$$V_s = \sqrt{\frac{G}{\rho}} \tag{2}$$

$$V_p = \sqrt{\frac{G(2-2v)}{\rho(1-2v)}} \tag{3}$$

where G , ρ , and v are shear modulus, density, and Poisson’s ratio of soils, respectively. In this study, we assumed v is 0.3 for soils, therefore:

$$\frac{V_p}{V_s} = 1.87 \tag{4}$$

The period for the horizontal seismic load T is:

$$T = \frac{2\pi}{\omega} = \frac{4H}{V_s} \tag{5}$$

α_h and α_v are horizontal and vertical seismic acceleration, respectively. We assumed that the direction of propagation of seismic waves is vertical. Then the acceleration of z deep location from the surface of the retaining wall at moment t is:

$$\alpha_h(z, t) = \alpha_h \times \sin\left[\omega\left(t - \frac{H-z}{V_s}\right)\right] \tag{6}$$

$$\alpha_v(z, t) = \alpha_v \times \sin\left[\omega\left(t - \frac{H-z}{V_p}\right)\right] \tag{7}$$

The body mass of the element in z with m depth and dz height $m_i(z)$ is:

$$m_i(z) = \frac{\gamma}{g} \times \frac{H-z}{\tan \alpha_i} \times dz, \tag{8}$$

while the self-weight of the i th slice is:

$$W_i = \gamma \times \left(\frac{l_i + l_{i+1}}{2}\right) \times dz \tag{9}$$

where γ is the unit weight of backfill soil, and l_i and l_{i+1} are the length of the top and bottom side of the i th slice, respectively.

Horizontal inertia force on the i th element is:

$$q_{hi} = m_i(z) \times \alpha_h(z, t) \tag{10}$$

Then the total horizontal seismic load on the slice Q_h is:

$$\begin{aligned} Q_h &= \int_0^H q_{hi} dz = \int_0^H m_i(z) \times \alpha_h(z, t) dz = \int_0^H \frac{\gamma}{g} \times \frac{H-z}{\tan \alpha_i} \times \alpha_h \times \sin\left[\omega\left(t - \frac{H-z}{V_s}\right)\right] dz \\ &= \frac{\lambda \times \gamma \times k_h}{4\pi^2 \tan \alpha_i} [2\pi H \cos \omega \xi + \lambda (\sin \omega \xi - \sin \omega t)] \end{aligned} \tag{11}$$

The vertical inertia force on the i th element is:

$$q_{vi} = m_i(z) \times \alpha_v(z, t) \tag{12}$$

Then the total horizontal seismic load on the retaining wall Q_v is

$$\begin{aligned} Q_v &= \int_0^H q_{vi} dz = \int_0^H m_i(z) \times \alpha_v(z, t) dz = \int_0^H \frac{\gamma}{g} \times \frac{H-z}{\tan \alpha_i} \times \alpha_v \times \sin\left[\omega\left(t - \frac{H-z}{V_p}\right)\right] dz \\ &= \frac{\lambda \times \gamma \times k_v}{4\pi^2 \tan \alpha_i} [2\pi H \cos \omega \psi + \lambda (\sin \omega \psi - \sin \omega t)] \end{aligned} \tag{13}$$

where λ is the vertical wavelength of the shear wave ($\lambda = T \times V_s$), and η denotes the vertical wavelength of the compression wave ($\xi = t - \frac{H}{V_s}$; $\psi = \frac{H}{V_p}$). By considering q_{hi} and q_{vi} on the critical direction of the element, the limits of Q_h and Q_v according to Ling and Leshchinsky [14] are, respectively:

$$\lim_{v_s \rightarrow \infty} (Q_h)_{\max} = \frac{\gamma \times H^2 \times \alpha_h}{2g \times \tan \alpha} = \frac{\alpha_h}{g} \times W = k_h \times W \tag{14}$$

$$\lim_{v_p \rightarrow \infty} (Q_v)_{\max} = \frac{\gamma \times H^2 \times \alpha_v}{2g \times \tan \alpha} = \frac{\alpha_v}{g} \times W = k_v \times W \tag{15}$$

where $k_h = \alpha_h/g$ and $k_v = \alpha_v/g\bar{X}$. When the i th slice is in limited equilibrium state, the vertical and horizontal stress applied on the slice are $\sum F_y = 0$ and $\sum F_x = 0$ [21,24], then:

$$F_{N,i+1} - F_{N,i} - W_i - Q_{v,i} + N_{t,i} \times \sin \alpha_i + N_{N,i} \times \cos \alpha_i = 0 \tag{16}$$

$$\sum_{i=1}^n T_i + \sum_{i=1}^n N_{t,i} \times \cos \alpha_i - \sum_{i=1}^n N_{N,i} \times \sin \alpha_i - \sum_{i=1}^n Q_{h,i} = 0 \tag{17}$$

4. Tensile Force of Reinforcement

According to the definition of safety factor [21], the shear force at the base of the slice is calculated by Equation (18):

$$N_{t,i} = \frac{1}{F_s} \times (c \times l_i + N_{N,i} \tan \varphi) \tag{18}$$

where c and φ are cohesion and friction angle of soil, respectively. The following formula can be obtained by compiling Equations (16) and (18):

$$N_{N,i} = \frac{F_{N,i} + W_i + Q_{v,i} - F_{N,i+1} - \frac{\sin \alpha_i \times c \times l_i}{F_s}}{\frac{\tan \varphi}{F_s} \times \sin \alpha_i + \cos \alpha_i} \tag{19}$$

Then Equation (19) can be obtained by compiling Equations (17)–(19):

$$\sum_{i=1}^n T_i + \sum_{i=1}^n \frac{1}{F_s} (c \times l_i + N_{N,i} \times \tan \varphi) - \sum_{i=1}^n Q_{h,i} - \sum_{i=1}^n \frac{F_{N,i} + W_i + Q_{v,i} - F_{N,i+1} - \frac{\sin \alpha_i \times c \times l_i}{F_s}}{\frac{\tan \varphi}{F_s} \times \sin \alpha_i + \cos \alpha_i} \times \sin \alpha_i = 0 \tag{20}$$

After that, the tensile force of reinforcement is:

$$\sum_{i=1}^n T_i = Q_h - \frac{c \times H \times \cos \alpha_i}{F_s \times \sin \alpha_i} - \frac{[\frac{\cos \alpha_i \times \tan \varphi}{F_s} - \sin \alpha_i] - [F_{N,0} + W + Q_v - \frac{c \times H}{F_s}]}{\frac{\sin \alpha_i \times \tan \varphi}{F_s} + \sin \alpha_i} \tag{21}$$

For each layer of reinforcement, the tensile force is:

$$T_i = K \times \gamma \times h_j \times S_{y,j} \tag{22}$$

where $S_{y,j}$ is the vertical distance between reinforcements and h_j denotes the vertical distance between the j th reinforcement and the top of the wall. The normalized tensile force K for all reinforcements is [21]:

$$K = \frac{\sum_{i=1}^n T_i}{0.5\gamma H^2} \tag{23}$$

For the stability analysis of a reinforced retaining wall under seismic loads [35], the maximum tensile force of each reinforcement needs to be calculated by Equation (22). This is also to determine the most critical log spiral slip surface, in which α_i is obtained. This problem is the optimal solution of the linear programming problem. Matlab was used to get the interactive solution of $\sum_{i=1}^n T_i$ and α_i .

5. Parametric Study

Figure 3 shows the geometry of the reinforced retaining wall as a case study. It can be seen that the wall is 6 m in height (H). The retaining wall is made of 6 pieces of reinforced concrete panel, each of which has a height of 1 m. The toe of the wall is made of plain concrete, with a width of 0.6 m and buried depth of 0.6 m. The reinforcement is made of metal, with a cross-section of 3×0.2 cm. Peak seismic acceleration α_{\max} is assumed to be 0.2 g. Factors affecting the stability of the retaining wall investigated are seismic acceleration coefficients (k_h and k_v) and soil parameters (c , γ , and φ); parameters for the study can be seen in Table 1.

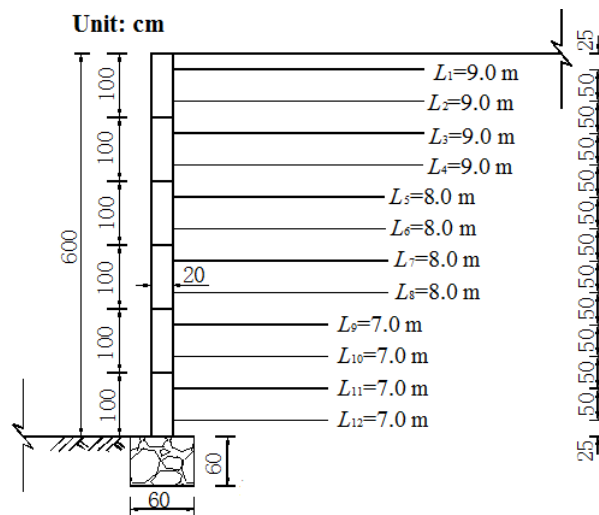


Figure 3. Geometry of the reinforced retaining wall.

Table 1. Geometric and geotechnical characteristics of the wall used for the parametric study.

Characteristics	Value	Average Value
Reinforced retaining wall height (<i>H</i>)	6 m	—
Soil density (γ)	16–21 kN/m ³	18.5 kN/m ³
Soil cohesion (<i>c</i>)	0–15 kN/m ²	10 kN/m ²
Internal angle of soil friction (φ)	28–38°	33°
Coefficient of horizontal seismic acceleration (k_h)	0, 0.1, 0.2, 0.3	0.15
Coefficient of vertical seismic acceleration (k_v)	0, 0.05, 0.1, 0.15	0.075

Note: The effect of soil’s relative density on the friction angle has not been taken into account.

5.1. Influence of Seismic Acceleration Coefficients

Variation of the normalized tensile force *K* with friction angle was also evaluated for various seismic acceleration coefficients. γ is fixed as 20 kN/m³, while *c* is treated as 0. The horizontal seismic acceleration coefficient k_h [36] is calculated by:

$$k_h = \frac{1}{2} \left(\frac{\alpha_{\max}}{g} \right), \tag{24}$$

while k_h and k_v need to fulfill the relationship of:

$$\varphi > \tan^{-1} \left(\frac{k_h}{1 - k_v} \right) \tag{25}$$

Figures 4 and 5 show the influence of seismic acceleration coefficients on the normalized tensile force, while Figure 6 illustrates the influence of seismic acceleration coefficients on the inclination angle. It can be identified that normalized tensile force increases with the increase of seismic acceleration coefficient, especially when k_h is increased from 0.1 to 0.2. Comparing Figure 4; Figure 5 shows that k_v also contributes to *K*, but it only has limited effect. This implies that the horizontal seismic load is the dominant force for a reinforced retaining wall. It also shows that when the friction angle increases, the normalized tensile force will decrease. This means that the use of a well-graded backfill material with a large friction angle will be beneficial to the stability of the reinforced retaining wall under seismic loads [37]. Figure 6 shows that the slip surface is almost linear from the toe to the middle part of the wall, since the variation of the inclination angle for each slice is very small, while from the middle to the top surface of the wall, the slip surface is a vertical line parallel to the wall. It also shows that the slip surface of the retaining wall moves toward the wall side with the increasing seismic load.

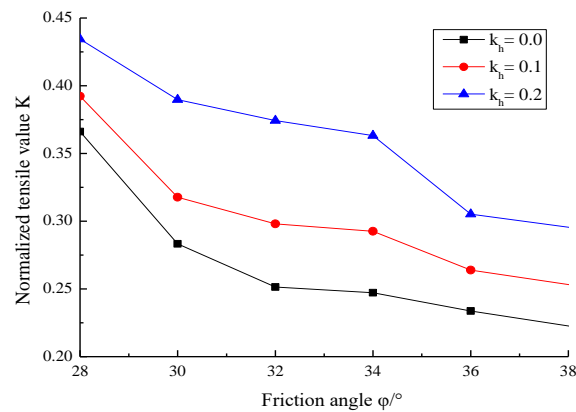


Figure 4. Normalized tensile force of reinforcement under seismic load when $k_v = 0$.

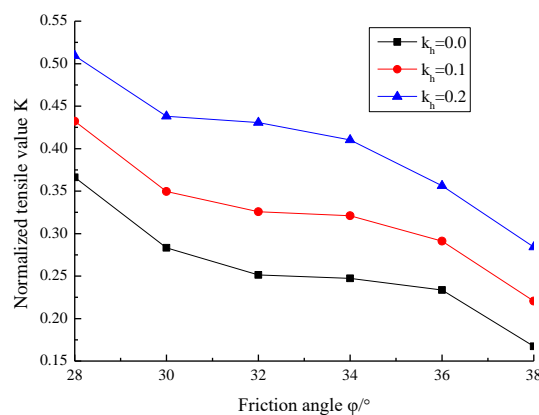


Figure 5. Normalized tensile force of reinforcement under seismic load when $k_v = 0.5 k_h$.

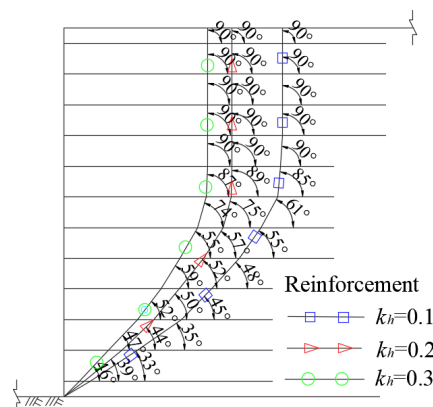


Figure 6. Inclination angle of slip surface and horizontal direction for various k_h .

5.2. Influence of Soil Parameters

Figure 7 shows the influence of cohesion of soil on normalized tensile force ($k = 0.5 k_h$, $\gamma = 20 \text{ kN/m}^3$, $\phi = 33^\circ$), while Figure 8 illustrates the influence of cohesion of soil on the inclination angle. It shows that with increased soil cohesion, the normalized tensile force tends to increase, and its increment is obvious. It can be identified from Figure 8 that the slip surface of the retaining wall moves toward the wall side with increasing cohesion. To investigate the effect of soil unit weight, soil cohesion and friction angle are fixed at 10 kPa and 33° , respectively, $k = 0.5$, and $k = 0.2$. It can be seen in Figure 9 that bigger unit weight leads to higher normalized tensile force. This implies that better stability of the retaining wall will be achieved by using lightweight backfill materials. Figure 10 illustrates that the slip surface of the retaining wall moves toward the wall side with increasing soil unit weight. Figure 11

shows the influence of soil friction angle on normalized tensile force ($k = 0.5, k = 0.2, \gamma = 20 \text{ kN/m}^3, c = 10 \text{ kPa}$), and that normalized tensile force decreases with the increased soil friction angle. Therefore, increasing the soil friction angle (such as by using some coarse materials) will contribute to the stability of the retaining wall. As demonstrated in Figure 12, the slip surface of the retaining wall moves toward the wall side with increments of friction angle.

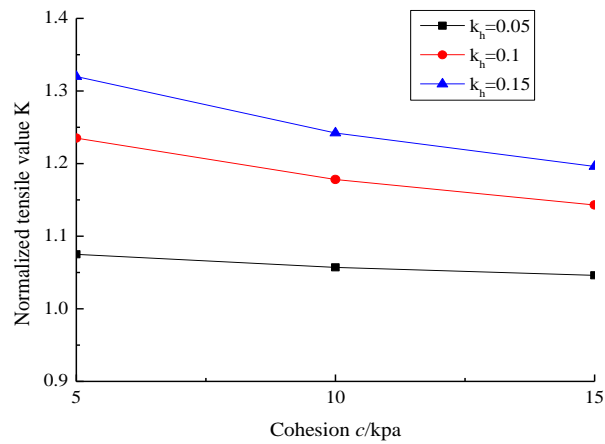


Figure 7. Effect of cohesion on normalized tensile force of reinforcement.

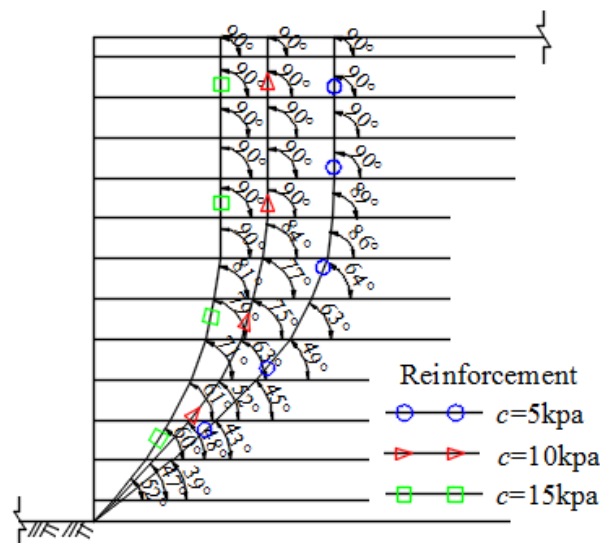


Figure 8. Inclination angle of slip surface and horizontal direction for various levels of cohesion.

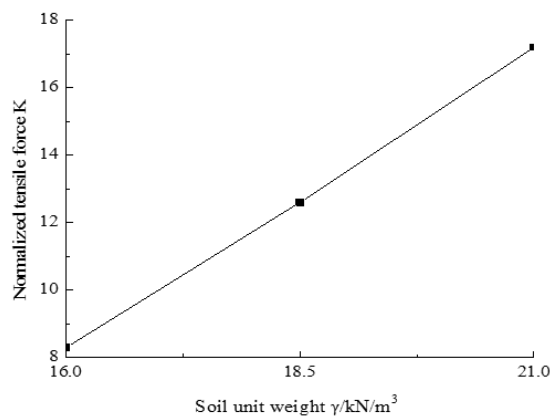


Figure 9. Effect of soil unit weight on normalized tensile force of reinforcement.

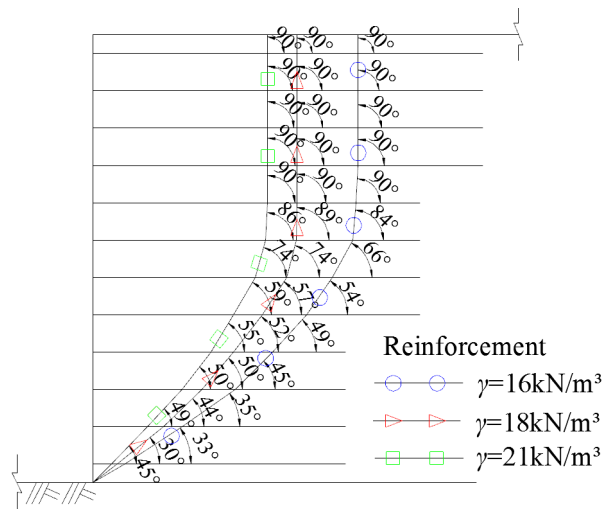


Figure 10. Inclination angle of slip surface and horizontal direction for various unit weights.

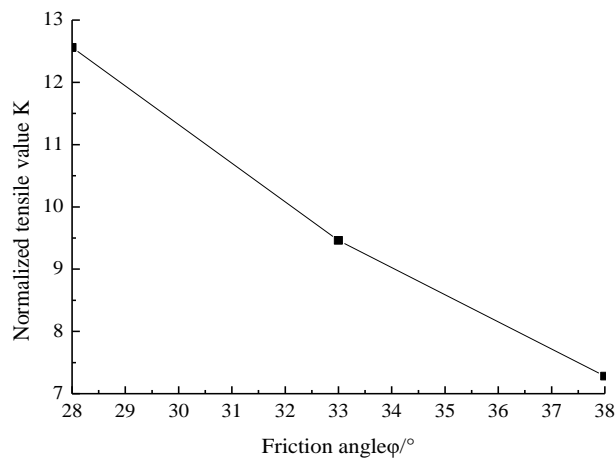


Figure 11. Effect of soil friction angle on normalized tensional force of reinforcement.

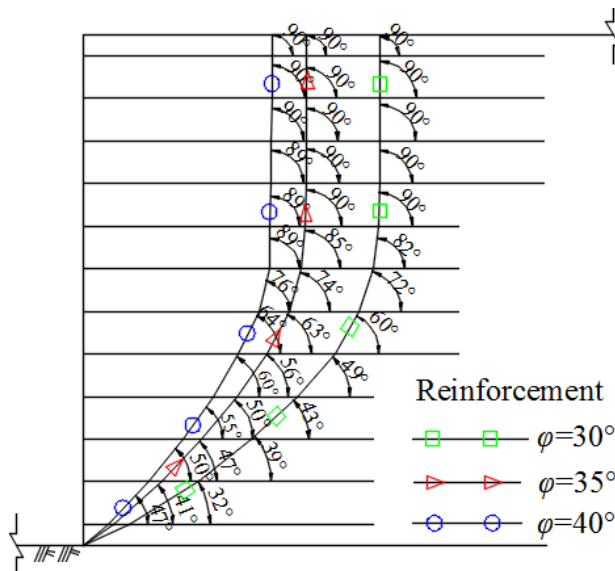


Figure 12. Inclination angle of slip surface and horizontal direction for various friction angles.

5.3. Influence of the Reinforcing Structure

Vertical distance between reinforcements ($S_{y,j}$) is the main parameter influencing the tensile force of the reinforcement. It can be identified from Equation (22) that tensile force has a positive relationship with the vertical distance between reinforcements. In other words, the tensile force will increase with increasing vertical distance between reinforcements. Thus, reducing the vertical distance between reinforcements is beneficial to reduce the tensile force, which is favorable for wall stability. Equation (22) also indicates that the reinforcing structure will not have a direct impact on the slip surface of the retaining wall.

5.4. Discussion

Based on a parametric analysis of the tensile force of reinforcement in a retaining wall, it can be seen that the horizontal seismic load, the vertical distance between reinforcements, and the soil friction angle are the three dominant factors influencing the tensile force. The findings are in agreement with Saeed and Ali [38] and Nouri et al. [23,32,39]. Vertical seismic load and soil cohesion have an insignificant impact on the tensile force of reinforcement, which is also close to the conclusions drawn by Nimbalkar et al. [34], Syed et al. [40], and Chandaluri et al. [41]. In summary, the HSM method adopted in this study could lead to similar results from a pseudostatic or experimental approach in previous research, proving that this method is suitable for analyzing the tensile force of reinforcement in retaining walls under seismic loads.

6. Conclusions

The horizontal slice method was adopted to analyze the stability of the reinforced retaining wall under seismic loads, while the slip surface was assumed to have a log spiral shape. Formulas for calculating the tensile force of reinforcement were established in this study. Parametric studies revealed that normalized tensile force increases with increased seismic acceleration coefficient and soil unit weight, while the tensile force of reinforcement will decrease with the increment of soil friction angle. Moreover, the influence of soil cohesion on normalized tensile force is not significant. Regarding the log spiral slip surface, it looks similar in various cases. It is almost linear from the toe to the middle part of the wall, since the variation of the inclination angle for each slice is very small, while from the middle to the top surface, it is a vertical line parallel to the wall. The slip surface of the retaining wall will move toward the wall side with increasing seismic load, soil cohesion, unit weight, or friction angle. The findings in this paper can provide theoretical basis and guidance for the design of reinforced retaining wall, and they could also strengthen the safety management of a reinforced retaining wall by considering earthquake conditions.

Author Contributions: The authors confirm their contributions to the paper as follows: L.J. and S.H. proposed the idea and wrote the paper; N.L. revised the manuscript; W.W. and K.Y. reviewed the results and approved the final version of the manuscript.

Funding: This research was funded by the National Natural Science Foundation of China (grant numbers 51568044, 41772311) and the Zhejiang Provincial Natural Science Foundation of China (grant number LY17E080016).

Acknowledgments: The Program of Study Abroad for Middle Age and Young Scholars supported by Lanzhou University of Technology is also acknowledged.

Conflicts of Interest: The authors declare no conflict of interest.

Nomenclature

$S_{t,i}$	shear force acting on the i th slice	τ_f	shear strength on the sliding surface
$N_{N,i}$	normal force acting on the i th slice	τ_r	shear stress on the sliding surface
l_{ai}	length of reinforcement in the slip zone behind the wall	k_v	vertical seismic coefficient
l_{ei}	length of reinforcement in the anchorage zone	k_h	horizontal seismic coefficient
$F_{N,i}$	normal force acting on the top of the i th slice	α_h	horizontal seismic acceleration
$F_{N,i+1}$	normal force acting on the bottom of the i th slice	α_v	vertical seismic acceleration
Q_{hi}	horizontal seismic force acting on the top of the slice	H	height of wall
Q_{vi}	vertical seismic force acting on the top of the slice	$\sum_{i=1}^n T_i$	maximum sum of forces to maintain stability of the reinforced wall
α_i	inclination angle of slip surface of the slice and horizontal direction	T_i	tensile force of i th layer reinforcement
W_i	weight of the i th slice	K	normalized form of required total force $\sum_{i=1}^n T_i$ to maintain stability of the wall
$S_{y,j}$	vertical distance between reinforcements	γ	soil density
n	number of reinforcement layers	φ	soil friction angle
F_s	safety for each slice	c	soil cohesion
h_j	vertical distance between j th reinforcement and the top of the wall		

References

- Bathurst, R.J.; Hatami, K. Seismic response analysis of a geosynthetic-reinforced soil retaining wall. *Geosynth. Int.* **1998**, *5*, 127–166. [[CrossRef](#)]
- Chen, Y.; Zhao, W.; Jia, P.J.; Han, J.Y.; Guan, Y.P. Dynamic behavior of an embedded foundation under horizontal vibration in a poroelastic half-space. *Appl. Sci.* **2019**, *9*, 740. [[CrossRef](#)]
- Subramaniam, P.; Banerjee, S. Factors affecting shear modulus degradation of cement treated clay. *Soil Dyn. Earthq. Eng.* **2014**, *65*, 181–188. [[CrossRef](#)]
- Ngo, V.L.; Kim, J.M.; Chang, S.H.; Lee, C. Effect of height ratio and mass ratio on structure-soil-structure interaction of two structures using centrifugal experiment. *Appl. Sci.* **2019**, *9*, 526. [[CrossRef](#)]
- Liu, S.Q.; Huang, X.W.; Zhou, A.Z.; Hu, J.; Wang, W. Soil-rock slope stability analysis by considering the non-uniformity of rocks. *Math. Probl. Eng.* **2018**, *2018*, 3121604. [[CrossRef](#)]
- Qin, C.; Chian, S.C. New perspective on seismic slope stability analysis. *Int. J. Geomech.* **2018**, *18*, 06018013. [[CrossRef](#)]
- Lu, W.H.; Miao, L.C.; Zhang, J.H.; Zhang, Y.X.; Li, J. Characteristics of deformation and damping of cement treated and expanded polystyrene mixed lightweight subgrade fill under cyclic load. *Appl. Sci.* **2019**, *9*, 167. [[CrossRef](#)]
- Zhang, L.; Goh, S.H.; Liu, H. Seismic response of pile-raft-clay system subjected to a long-duration earthquake: Centrifuge test and finite element analysis. *Soil Dyn. Earthq. Eng.* **2017**, *92*, 488–502. [[CrossRef](#)]
- Zhang, L.; Liu, H. Seismic response of clay-pile-raft-superstructure systems subjected to far-field ground motions. *Soil Dyn. Earthq. Eng.* **2017**, *101*, 209–224. [[CrossRef](#)]
- Liu, Y.; Zhang, L. Seismic response of pile-raft system embedded in spatially random clay. *Géotechnique* **2018**. [[CrossRef](#)]
- Okabe, S. General theory on earth pressure and seismic stability of retaining wall and dam. *J. Jpn. Soc. Civ. Eng.* **1924**, *10*, 1277–1323.
- Basha, B.M.; Babu, G.S. Seismic rotational displacements of gravity walls by pseudodynamic method with curved rupture surface. *Int. J. Geomech.* **2009**, *10*, 93–105. [[CrossRef](#)]
- Zeng, X.; Steedman, R.S. On the behaviour of quay walls in earthquakes. *Géotechnique* **1993**, *43*, 417–431. [[CrossRef](#)]
- Ling, H.I.; Leshchinsky, D. Effects of vertical acceleration on seismic design of geosynthetic-reinforced soil structures. *Géotechnique* **1998**, *48*, 347–373. [[CrossRef](#)]

15. Kwak, C.; Park, J.; Jang, D.; Park, I. Dynamic shear degradation of geosynthetic–soil interface in waste landfill sites. *Appl. Sci.* **2017**, *7*, 1225. [[CrossRef](#)]
16. Shahgholi, M.; Fakher, A.; Jones, C.J.F.P. Horizontal slice method of analysis. *Géotechnique* **2001**, *51*, 881–885. [[CrossRef](#)]
17. Choudhury, D.; Singh, S. New approach for estimation of static and seismic active earth pressure. *Geotech. Geol. Eng.* **2006**, *24*, 117–127. [[CrossRef](#)]
18. El-Emam, M.M.; Bathurst, R.J. Experimental design, instrumentation and interpretation of reinforced soil wall response using a shaking table. *Int. J. Phys. Model. Geotech.* **2004**, *4*, 13–32. [[CrossRef](#)]
19. Guler, E.; Enunlu, A.K. Investigation of dynamic behavior of geosynthetic reinforced soil retaining structures under earthquake loads. *Bull. Earthq. Eng.* **2009**, *7*, 737–777. [[CrossRef](#)]
20. Jia, L.; Zhu, Y.; Lai, C. Stability analysis of reinforced earth retaining wall under earthquake. *J. Southwest Jiao Tong Univ.* **2016**, *51*, 698–703. (In Chinese)
21. Jia, L.; Guo, J.; Yao, K. Seismic stability analysis of reinforced soil slope using horizontal slice method. *J. Basic Sci. Eng.* **2018**, *26*, 168–176. (In Chinese)
22. Lo, S.R.; Xu, D.W. A strain-based design method for the collapse limit state of reinforced soil walls or slopes. *Can. Geotech. J.* **1992**, *29*, 832–842. [[CrossRef](#)]
23. Nouri, H.; Fakher, A.; Jones, C.J.F.P. Development of horizontal slice method for seismic stability analysis of reinforced slopes and walls. *Geotext. Geomembr.* **2006**, *24*, 175–187. [[CrossRef](#)]
24. Jiang, J.; Yang, G. A New Slice Method for Seismic Stability Analysis of Reinforced Retaining Wall. In *Computational Structural Engineering*; Springer: Dordrecht, The Netherlands, 2009; pp. 167–172.
25. Lin, Y.-L.; Leng, W.-M.; Yang, G.-L.; Zhao, L.-H.; Li, L.; Yang, J.-S. Seismic active earth pressure of cohesive-frictional soil on retaining wall based on a slice analysis method. *Soil Dyn. Earthq. Eng.* **2015**, *70*, 133–147. [[CrossRef](#)]
26. Gao, Y.; Yang, C.; Wu, Y.; Li, D.; Zhang, F. Evaluation of oblique pullout resistance of reinforcements in soil wall subjected to seismic loads. *Geotext. Geomembr.* **2014**, *42*, 515–524. [[CrossRef](#)]
27. Lin, Y.; Cheng, X.; Yang, G. Shaking table test and numerical simulation on a combined retaining structure response to earthquake loading. *Soil Dyn. Earthq. Eng.* **2018**, *108*, 29–45. [[CrossRef](#)]
28. Cakir, T. Evaluation of the effect of earthquake frequency content on seismic behavior of cantilever retaining wall including soil–structure interaction. *Soil Dyn. Earthq. Eng.* **2013**, *45*, 96–111. [[CrossRef](#)]
29. Peng, J.; Zhu, Y.; Zhou, Y. Derivation of Shukla’s generalized expression of seismic passive earth pressure on retaining walls with cohesive-frictional backfill by the inclined slice element method. *Soil Dyn. Earthq. Eng.* **2018**, *114*, 225–228. [[CrossRef](#)]
30. Trandafir, A.C.; Kamai, T.; Sidle, R.C. Earthquake-induced displacements of gravity retaining walls and anchor-reinforced slopes. *Soil Dyn. Earthq. Eng.* **2009**, *29*, 428–437. [[CrossRef](#)]
31. Askari, F.; Totonchi, A.; Farzaneh, O. Application of admissible stress fields for computation of passive seismic force in retaining walls. *Sci. Iran.* **2012**, *19*, 967–973. [[CrossRef](#)]
32. Nouri, H.R.; Fakher, A. The Effect of Amplification on the Seismic Stability of Reinforced Soil Slopes Using Horizontal Slice Method. *Geotech. Earthquake Eng. Soil Dyn. IV* **2008**, 1–10. [[CrossRef](#)]
33. Ahmad, S.M.; Choudhury, D. Pseudo-dynamic approach of seismic design for waterfront reinforced soil-wall. *Geotext. Geomembr.* **2008**, *26*, 291–301. [[CrossRef](#)]
34. Nimbalkar, S.S.; Choudhury, D.; Mandal, J.N. Seismic stability of reinforced soil-wall by pseudo-dynamic method. *Geosynth. Int.* **2006**, *13*, 111–119. [[CrossRef](#)]
35. Reddy, G.N.; Madhav, M.R.; Reddy, E.S. Pseudo-static seismic analysis of reinforced soil wall—Effect of oblique displacement. *Geotext. Geomembr.* **2008**, *26*, 393–403. [[CrossRef](#)]
36. Boulanger, R.W. Seismic Design Guidelines for Port Structures. *Earthq. Spectra* **2002**, *18*, 579–580. [[CrossRef](#)]
37. GuhaRay, A.; Baidya, D.K. Reliability coupled sensitivity-based seismic analysis of gravity retaining wall using Pseudostatic approach. *J. Geotech. Geoenviron. Eng.* **2016**, *142*, 04016010. [[CrossRef](#)]
38. Shekarian, S.; Ghanbari, A. A pseudo-dynamic method to analyze retaining wall with reinforced and unreinforced backfill. *J. Seismol. Earthq. Eng.* **2008**, *10*, 41–46.
39. Nouri, H.; Fakher, A.; Jones, C.J.F.P. Evaluating the effects of the magnitude and amplification of pseudo-static acceleration on reinforced soil slopes and walls using the limit equilibrium Horizontal Slices Method. *Geotext. Geomembr.* **2008**, *26*, 263–278. [[CrossRef](#)]

40. Syed, M.; Deepankar, C. Seismic internal stability analysis of waterfront reinforced-soil wall using pseudo-static approach. *Ocean Eng.* **2012**, *52*, 83–90.
41. Chandaluri, V.K.; Sawant, V.A.; Shukla, S.K. Seismic Stability Analysis of Reinforced Soil Wall Using Horizontal Slice Method. *Int. J. Geosynth. Ground Eng.* **2015**, *1*, 23. [[CrossRef](#)]



© 2019 by the authors. Licensee MDPI, Basel, Switzerland. This article is an open access article distributed under the terms and conditions of the Creative Commons Attribution (CC BY) license (<http://creativecommons.org/licenses/by/4.0/>).